Solution Asymmetry and Salt Expand Fluid-Fluid Coexistence Regions of Charged Membranes

Bastian Kubsch,[1] Tom Robinson,[1] Reinhard Lipowsky,[1] and Rumiana Dimova[1,*]
[1]Max Planck Institute of Colloids and Interfaces, Potsdam, Germany

ABSTRACT   Liquid-liquid phase separation in giant unilamellar vesicles (GUVs) leads to the formation of intramembrane domains. To mimic charged biological membranes, we studied phase separation and domain formation in GUVs of ternary lipid mixtures composed of egg sphingomyelin, cholesterol, and the negatively charged lipid dioleoylphosphatidylglycerol. The GUVs were exposed to solutions of sucrose and high-saline buffer. The phase diagram was determined using epifluorescence microscopy for vesicle populations with symmetric and asymmetric solution compositions across the membranes. Trans-membrane solution asymmetry was found to affect the membrane phase state. Furthermore, compared to the case of salt-free conditions, the phase diagram in the presence of high-saline buffer (both symmetrically or asymmetrically present across the membrane) was found to exhibit a significantly extended region of liquid-ordered and liquid-disordered coexistence. These observations were confirmed on single GUVs using microfluidics and confocal microscopy. Moreover, we found that the miscibility temperatures markedly increased for vesicles in the presence of symmetric and asymmetric salt solutions. Our results demonstrate a substantial effect of salt and solution asymmetry on the phase behavior of charged membranes, which has direct implications for protein adsorption onto these membranes and for the repartitioning of proteins within the membrane domains.

In the fluid-mosaic model of Singer and Nicolson, the plasma membrane is viewed as a more or less homogeneous lipid bilayer decorated by membrane-anchored proteins. This view has been challenged with the extraction of detergent-resistant membrane domains from biological cells, a discovery that led to the lipid raft hypothesis proposing the existence of lipid domains that are rich in sphingomyelin and cholesterol (1,2). Even though this hypothesis has now been pursued for almost two decades, it is still a matter of ongoing debate (3–5). The different experimental techniques used to search for rafts in biological membranes have been recently reviewed (6). One important result of this activity was the identification of ternary lipid mixtures, which undergo phase separation into liquid-disordered (L_d) and liquid-ordered (L_o) phases and can be directly observed in giant unilamellar vesicles (GUVs) (7) using fluorescence microscopy (8).

This type of phase separation has now been examined in numerous studies in which the GUVs were prepared in nonphysiological buffers such as pure water, sucrose, or low-saline solution (9–13). Here, we studied the phase behavior of lipid bilayers under high-saline physiological conditions. Because different GUV dispersion media can significantly alter physical membrane properties such as the bending rigidity (14,15), we addressed the question of how high-saline buffers influence the lipid phase state of GUVs. Similar investigations with charged vesicles in low-saline buffers resulted in rather small effects (11,12,16). On the other hand, neutral membranes in salt-free conditions (17) and exposed to saline buffers in the vesicle exterior (18) seem to differ in their phase behavior.

Here, we first compared the phase states of charged GUVs with membranes symmetrically exposed (inside and outside) to sucrose solution or high-saline buffer. We also investigated GUVs exposed to asymmetric conditions with sucrose solution and high-saline buffer on either side of the membrane. Solution asymmetry across plasma membranes is not only biologically relevant; implementing asymmetric solution conditions is also important in GUV-based studies. Examples include establishing, e.g., optical contrast or sucrose/glucose density gradients (11,13) and mimicking the native environment for proteins (13,19,20).

We analyzed the phase state of charged multicomponent GUVs via fluorescence microscopy. Vesicles were prepared from negatively charged DOPG (dioleoylphosphatidylglycerol), eSM (egg sphingomyelin), and Chol (cholesterol), in either sucrose (210 mOsm/kg) or high-saline buffer

---

(100 mM NaCl, 10 mM Tris, pH 7.5, 210 mOsm/kg) using spontaneous swelling; see the Supporting Material for GUV preparation and visualization. As a fluorescent marker, GUVs additionally contained 0.1 mol% of $DiIC_{18}$, which is known to preferentially partition into the L_d phase and to be excluded from the L_o and solid (S) phases (21).

The phase diagram of GUVs symmetrically exposed to sucrose solution or salt buffer at ~23°C contains one-phase fluid, liquid-liquid, and solid-liquid coexistence regions (Fig. 1, A and C). Membrane domains always appeared to be in registration, i.e., the domains in the outer and inner leaflets were spatially matched. Differences from observations with the same ternary system (11) may be ascribed to a different method of vesicle preparation as well as to the differences in solution compositions (12). Notably, compared to symmetric sucrose conditions, the L_o/L_d coexistence region of GUVs is increased for symmetric salt conditions (compare *upper parts* of Fig. 1, A and C).

The region of lipid compositions showing different phase behaviors under symmetric conditions in either sucrose solution or salt buffer were reinvestigated with asymmetrically distributed solutions on either side of the membrane. GUVs initially grown in the internal solution were 20-fold diluted with the desired external solution (corresponding to a 95% external solution exchange). Phase states remained the same for all but two of the examined compositions going from symmetric salt buffer to salt buffer inside and sucrose solution outside the vesicle (Fig. 1 C). In the opposite case, however, the exchange from symmetric sucrose solution to sucrose solution inside and salt buffer outside changed the GUV phase state to that of the symmetric salt buffer conditions for most compositions (Fig. 1 A). Note that the same phase behavior of asymmetrically exposed membranes

was found for both salt/sugar and sugar/salt in/out asymmetry, as expected.

These bulk observations were corroborated by studies on single GUVs trapped in a microfluidic device (22). This approach not only allows us to track individual GUVs but also to fully exchange the external solution. Vesicles consisting of 30:40:30 DOPG/eSM/Chol (mol %) prepared in either sucrose solution or salt buffer were captured by microposts (see the Supporting Material for fabrication) and observed by confocal microscopy before a full external solution exchange was performed. As in the bulk, these vesicles were in the single-liquid state when prepared in symmetric sucrose solutions (Fig. 1 B, *top*) and exhibited L_o/L_d coexistence when prepared in symmetric salt buffer (Fig. 1 D, *top*). Observations after a full external solution exchange showed that vesicles prepared in symmetric sucrose solutions had a uniform lipid composition but underwent L_o/L_d phase separation when exposed to salt buffer outside (Fig. 1 B, *bottom*). On the other hand, vesicles prepared in salt buffer and exposed to sucrose solution outside remained phase-separated as for symmetric salt conditions (Fig. 1 D, *bottom*). It was also possible to reach a homogeneous state with GUVs, which initially exhibited L_o/L_d coexistence (Fig. S1).

The increased L_o/L_d coexistence region in the presence of salt (Fig. 1) implies the stabilization of L_d domains with an increased fraction of the charged DOPG lipid. This was further tested by measuring the miscibility transition temperatures of GUVs prepared from 40:30:30 DOPG/eSM/Chol under different solution conditions (see Supporting Materials and Methods). In bulk observations at ~23°C, GUVs of this composition had a uniform lipid composition under symmetric sucrose conditions and exhibited L_o/L_d coexistence under symmetric salt
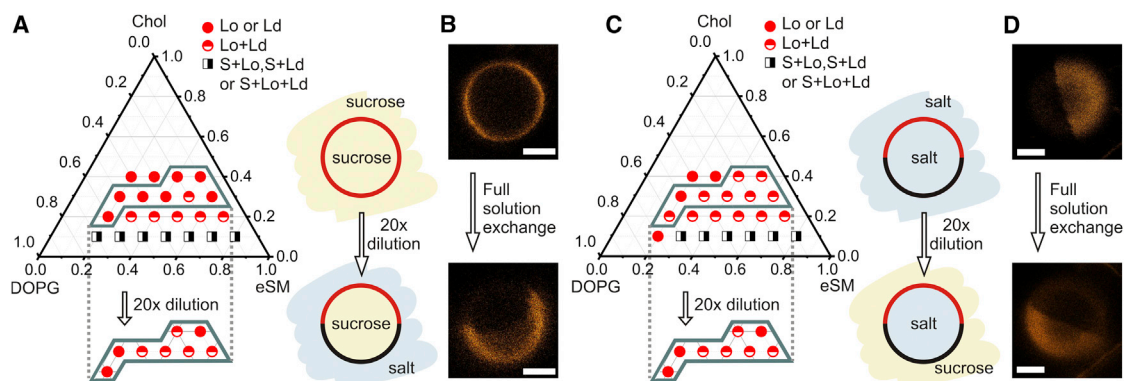

FIGURE 1 Effect of trans-membrane solution asymmetry on the phase behavior of DOPG/eSM/Chol. (*A*) Phase diagram for GUVs with symmetric sucrose/sucrose conditions; the lower polygonal section corresponds to asymmetric sucrose/salt (in/out) conditions after 20-fold dilution of the vesicle suspension with high-saline buffer. The cartoons illustrate the solution conditions and the dominant domain pattern within the highlighted section. (*B*) Confocal images of a single GUV (DOPG/eSM/Chol 30:40:30) captured within a microfluidic device before (*top*) and after (*bottom*) full exchange of the external solution from symmetric sucrose/sucrose to sucrose/salt (in/out). (*C*) Phase diagram for symmetric salt/salt conditions; the lower polygonal section is obtained for asymmetric salt/sucrose (in/out) conditions after 20-fold dilution with sucrose solution. As in (*A*), the cartoons illustrate solution conditions and the dominant domain pattern within the highlighted section. (*D*) Confocal images of a single GUV (DOPG/eSM/Chol 30:40:30) before (*top*) and after (*bottom*) the full exchange of the external solution from symmetric salt/salt to asymmetric salt/sucrose (in/out). Scale bars, 3 μm.
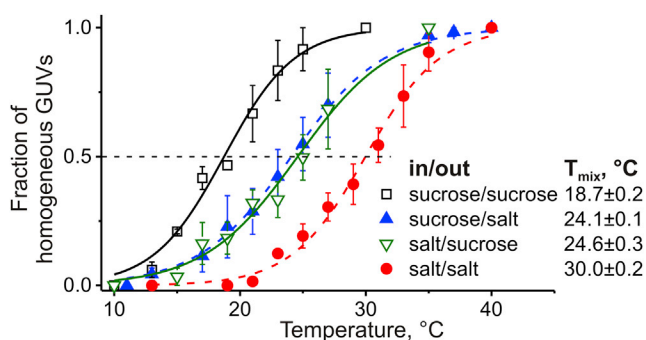
FIGURE 2 L_o/L_d miscibility transition curves for 40:30:30 DOPG/eSM/Chol vesicles under different solution conditions. Data were fitted using the Boltzmann model (see the Supporting Material), where T_{mix} was deduced from the half-maximum indicated by the dashed line. Error bars represent the standard error of the mean of three independent experiments. To see this figure in color, go online.

direct implications for protein adsorption and domain repartitioning.

SUPPORTING MATERIAL

Supporting Materials and Methods and one figure are available at http://www.biophysj.org/biophysj/supplemental/S0006-3495(16)30353-8.

AUTHOR CONTRIBUTIONS

B.K., T.R., R.L., and R.D. designed the experiments; B.K. and T.R. performed the experiments and analyzed the results; and all authors wrote and edited the article.

ACKNOWLEDGMENTS

conditions. Fig. 2 summarizes the miscibility transition temperatures, T_{mix}, for all symmetric and asymmetric conditions. While T_{mix} is lowest for symmetric sucrose, it increases with salt present on one side of the membrane and is highest for salt symmetrically distributed on both sides of the membrane. We showed that both symmetric and asymmetric high-saline conditions for the two leaflets of charged GUV membranes have a substantial effect on their phase behavior. Together with the expanded L_o/L_d coexistence region of the GUV phase diagrams, the increase of the miscibility transition temperatures implies that salt leads to the stabilization of domains with an increased fraction of DOPG.

Previously, the presence of salt was shown to alter DOPG mobility in membranes because of screening of the head-group charges (23). The effect of asymmetric ionic solutions on the phase diagram of binary lipid mixtures has also been studied using Poisson-Boltzmann theory (24). High salt concentrations decrease the Debye length, thereby reducing the energetic cost for the dense packing of charges. This allows for L_d domains enriched in DOPG to form, thus expanding the L_o/L_d coexistence region and raising the miscibility temperature. This explanation for the observed effect of salt cannot be fully applied to the results obtained with asymmetric conditions, for which only one leaflet is exposed to salt. In principle, the salt-induced phase separation in this leaflet could propagate to the other leaflet, but another factor to consider is the spontaneous curvature generated in the membrane by the asymmetric solutions (25). Thus, it is important to study the interplay of spontaneous curvature and phase separation for multicomponent membranes under asymmetric solution conditions. Our study emphasizes that the precise buffer composition and trans-membrane solution asymmetry influence the membrane phase behavior, and should not be ignored when comparing available data. Furthermore, the effect of salt and solution asymmetry on the phase behavior of charged membranes might have

REFERENCES

1. Brown, D. A., and E. London. 1997. Structure of detergent-resistant membrane domains: does phase separation occur in biological membranes? *Biochem. Biophys. Res. Commun.* 240:1–7.

2. Simons, K., and E. Ikonen. 1997. Functional rafts in cell membranes. *Nature.* 387:569–572.

3. Lingwood, D., and K. Simons. 2010. Lipid rafts as a membrane-organizing principle. *Science.* 327:46–50.

4. Owen, D. M., A. Magenau, …, K. Gaus. 2012. The lipid raft hypothesis revisited—new insights on raft composition and function from super-resolution fluorescence microscopy. *BioEssays.* 34:739–747.

5. Goñi, F. M. 2014. The basic structure and dynamics of cell membranes: an update of the Singer-Nicolson model. *Biochim. Biophys. Acta.* 1838:1467–1476.

6. Klotzsch, E., and G. J. Schutz. 2013. A critical survey of methods to detect plasma membrane rafts. *Philos. Trans. Roy. Soc. B.* 368:20120033.

7. Dimova, R., S. Aranda, …, R. Lipowsky. 2006. A practical guide to giant vesicles. Probing the membrane nanoregime via optical microscopy. *J. Phys. Condens. Matter.* 18:S1151–S1176.

8. Dietrich, C., L. A. Bagatolli, …, E. Gratton. 2001. Lipid rafts reconstituted in model membranes. *Biophys. J.* 80:1417–1428.

9. Baumgart, T., S. T. Hess, and W. W. Webb. 2003. Imaging coexisting fluid domains in biomembrane models coupling curvature and line tension. *Nature.* 425:821–824.

10. Bacia, K., P. Schwille, and T. Kurzchalia. 2005. Sterol structure determines the separation of phases and the curvature of the liquid-ordered phase in model membranes. *Proc. Natl. Acad. Sci. USA.* 102:3272–3277.

11. Vequi-Suplicy, C. C., K. A. Riske, …, R. Dimova. 2010. Vesicles with charged domains. *Biochim. Biophys. Acta.* 1798:1338–1347.

12. Blosser, M. C., J. B. Starr, …, S. L. Keller. 2013. Minimal effect of lipid charge on membrane miscibility phase behavior in three ternary systems. *Biophys. J.* 104:2629–2638.

13. Pataraia, S., Y. G. Liu, …, R. Dimova. 2014. Effect of cytochrome *c* on the phase behavior of charged multicomponent lipid membranes. *Biochim. Biophys. Acta.* 1838:2036–2045.

14. Dimova, R. 2014. Recent developments in the field of bending rigidity measurements on membranes. *Adv. Colloid Interface Sci.* 208:225–234.

15. Bouvrais, H., L. Duelund, and J. H. Ipsen. 2014. Buffers affect the bending rigidity of model lipid membranes. *Langmuir.* 30:13–16.

16. Shimokawa, N., M. Hishida, …, K. Yoshikawa. 2010. Phase separation of a mixture of charged and neutral lipids on a giant vesicle induced by small cations. *Chem. Phys. Lett.* 496:59–63.

17. Bezlyepkina, N., R. S. Gracià, …, R. Dimova. 2013. Phase diagram and tie-line determination for the ternary mixture DOPC/eSM/cholesterol. *Biophys. J.* 104:1456–1464.

18. Carravilla, P., J. L. Nieva, …, N. Huarte. 2015. Two-photon Laurdan studies of the ternary lipid mixture DOPC:SM:cholesterol reveal a single liquid phase at sphingomyelin:cholesterol ratios lower than 1. *Langmuir.* 31:2808–2817.

19. Manneville, J. B., J. F. Casella, …, B. Goud. 2008. COPI coat assembly occurs on liquid-disordered domains and the associated membrane deformations are limited by membrane tension. *Proc. Natl. Acad. Sci. USA.* 105:16946–16951.

20. Wollert, T., C. Wunder, …, J. H. Hurley. 2009. Membrane scission by the ESCRT-III complex. *Nature.* 458:172–177.

21. Kahya, N., D. Scherfeld, …, P. Schwille. 2003. Probing lipid mobility of raft-exhibiting model membranes by fluorescence correlation spectroscopy. *J. Biol. Chem.* 278:28109–28115.

22. Robinson, T., P. Kuhn, …, P. S. Dittrich. 2013. Microfluidic trapping of giant unilamellar vesicles to study transport through a membrane pore. *Biomicrofluidics.* 7:44105.

23. Filippov, A., G. Orädd, and G. Lindblom. 2009. Effect of NaCl and $CaCl_2$ on the lateral diffusion of zwitterionic and anionic lipids in bilayers. *Chem. Phys. Lipids.* 159:81–87.

24. Shimokawa, N., S. Komura, and D. Andelman. 2011. Charged bilayer membranes in asymmetric ionic solutions: phase diagrams and critical behavior. *Phys. Rev. E Stat. Nonlin. Soft Matter Phys.* 84:031919.

25. Lipowsky, R. 2013. Spontaneous tubulation of membranes and vesicles reveals membrane tension generated by spontaneous curvature. *Faraday Discuss.* 161:305–331. discussion 419–459.

Supplemental Information

Solution Asymmetry and Salt Expand Fluid-Fluid Coexistence Regions of Charged Membranes

Bastian Kubsch, Tom Robinson, Reinhard Lipowsky, and Rumiana Dimova*

Max Planck Institute of Colloids and Interfaces, Science Park Golm, 14424 Potsdam, Germany

* Address reprint requests and inquiries to dimova@mpikg.mpg.de

Materials

1,2-dioleoyl-*sn*-glycero-3-phospho-(1'-*rac*-glycerol), sodium salt (DOPG), chicken egg sphingomyelin (eSM), and cholesterol (Chol, ovine wool, > 98 %) were purchased from Avanti Polar Lipids (Alabaster, IL). The fluorescent dye 1,1′-dioctadecyl-3,3,3′,3′-tetramethylindocarbocyanine perchlorate (DiIC$_{18}$) was acquired from Molecular Probes (Eugene, Oregon). Chloroform obtained from Merck (Darmstadt, Germany) was of HPLC grade (≥ 99.8 %). Polydimethylsiloxan (PDMS) and curing agent (Sylgard 184) were purchased from Dow Corning (Midland, Michigan). NaCl (> 99.8 %), HCl (37 %), and Tris (≥ 99.9 %) were from Roth (Karlsruhe, Germany). Sucrose (≥ 99.5 %) was obtained from Sigma-Aldrich (St. Louis, Missouri). Ultrapure water was used for all buffer preparations.

Preparation of GUVs

GUVs were prepared from a 4 mM lipid stock in chloroform containing different ratios of charged DOPG, eSM and Chol. As a fluorescent marker, the mixtures additionally contained 0.1 mol% of DiIC$_{18}$. Vesicles were grown by spontaneous swelling according to Ref. (1). Briefly, 10 – 15 µl of lipid stock were deposited on a clean ~1 cm² polytetrafluoroethylene (PTFE, known as Teflon) plate and desiccated under vacuum at 60 °C for 2 h. The dried lipid film was pre-swollen in a water-saturated atmosphere at the same temperature for 4 h. Finally, the film was hydrated with the growing solution, here, either 210 mM sucrose (210 mOsm/kg) or high-saline buffer composed of 100 mM NaCl, 10 mM Tris at pH 7.5 (210 mOsm/kg), and incubated at 60 °C overnight. After swelling, GUVs were cooled down to room temperature (~ 23 °C) within one hour. The vesicles accumulated in a red clump visible by eye during swelling which was harvested and re-suspended in 1 mL of the hydration solution. The sample was then ready for analysis of symmetric solution conditions. To create asymmetric solution conditions, GUVs were grown in the internal solution and diluted by 20 times in the desired external solution. Both solutions were osmotically matched (Osmomat 030, Berlin, Germany) before dilution. The vesicles were left for equilibration for at least 1 h before observation. Phase state observations of all solution conditions were performed on the day of GUV harvest.

GUV visualization and phase state assessment

For phase diagram mapping, epifluorescence microscopy was used. Per batch, 30 – 70 GUVs with no or minimal defects and a diameter larger than 5 µm were analyzed for their phase state. The whole batch was assigned the dominating majority phase state among the GUVs analyzed. In order to describe the phase state of vesicles, certain criteria were followed. The single-liquid state (Lo or Ld) was characterized by a homogeneous distribution of $DiIC_{18}$ throughout the entire vesicle which appeared spherical and smooth. The liquid-liquid coexistence state (Lo/Ld) was marked by the appearance of circular domains with smooth boundaries, which were free to diffuse. Solid-liquid coexistence states (S/Lo, S/Ld, S/Lo/Ld) featured angular, sometimes finger-like domains with static boundaries. If the solid domains dominate, vesicles showed an overall angular appearance. GUVs assigned to the Lo/Ld coexistence region were analyzed with a 40x/0.6 NA objective (Axio Observer.D1, Zeiss, Oberkochen, Germany), while those assigned to a solid-liquid coexistence state were observed via a 63x/1.2 NA water objective (TCS SP5, Leica, Wetzlar, Germany) due to their fine structures. GUVs of identical compositions but exposed to different solution conditions were always observed with the same objective to allow direct comparison. The visual assessment of phase states based on these criteria ensured correct comparisons across different solutions. Yet, for compositions yielding very small vesicles and/or small domains, judgments of phase states may vary among individual observers. Batch observations where ~50 % of vesicles were phase-separated (if composition close to the border between single-liquid and liquid/liquid regions) were repeated several times in independent experiments to judge the phase state. Analyses of phase states under asymmetric conditions were performed at least 3 times on independent batches in case an alteration was observed. The imaging of GUVs captured on the microfluidic device was done using confocal laser scanning microscopy with a 63x/1.2 NA objective (TCS SP5, Leica, Wetzlar, Germany).

GUV miscibility transition temperatures

To determine the miscibility temperatures, the vesicles were introduced into a custom-made chamber with temperature controlled by circulating water connected to a thermostat. During analysis, the temperature was increased by 2 °C every 5 – 10 min (depending on observation time required) until the vesicles in the investigated batch appeared homogenous. To check for hysteresis, a representative sample of GUVs with sucrose inside and outside was cooled down again after analysis. The fraction of phase separation was checked at $T = 19$ °C and $T = 13$ °C and was the same as during the period of temperature increase. Due to different density gradients in case of asymmetric solution conditions vesicles would float up to the cover glass or settle onto the microscope slide. Therefore, objective lenses with different working distances needed to be used, namely 40x/0.75 NA for short-distance and 63x/0.9 NA for long-distance. A control experiment was performed using both objectives to assess the phase state statistics and revealed no significant differences depending on the objective resolution and the location of the vesicles in the chamber. GUVs were incubated for at least 2 minutes at each temperature before observation. In order to assess the fraction of homogenous

membranes y, between 20 and 40 vesicles were analyzed at each temperature and in total 3 independent batches were analyzed. The resulting data were fitted to the sigmoidal Boltzmann function:

$$y = \frac{A_1 - A_2}{1 + e^{T - T_{mix}/dT}} + A_2 \tag{1}$$

where y represents the fraction of uniform GUVs, A_1 the fraction at the lowest temperature, A_2 the fraction at the highest temperature, T the temperature, and T_{mix} the temperature at half-maximal y. As y is the fraction of homogenous GUVs, A_1 and A_2 were fixed to 0 and 1, respectively, corresponding to the experimental situation. The miscibility transition was assumed to be sigmoidal and therefore once the fraction value was measured to be 0 at a certain temperature, all fraction values below that temperature were assumed to be 0. Vice versa, once the fraction value reached 1 at a particular temperature, all fraction values above this temperature were assumed to be 1.

Fabrication of the microfluidic device

The multi-layered PDMS microfluidic device was fabricated as previously described (2). The upper layer serves as a control layer to hydraulically actuate circular valves, while the lower layer contains the GUV solutions. Briefly, PDMS oligomer and curing agent were mixed at a ratio of 10:1 and poured onto the silicon wafer master for the upper layer (feature height: 20 µm) to a final thickness of 5 mm. The same PDMS mixture was spin coated onto the silicon wafer for the lower layer (feature height: 20 µm) at 2000 rpm to a height of 40 µm. Both were then cured at 80 °C for 3 h. The upper layer was then cut to size and 1 mm holes were punched using a 1 mm Biopsy puncher (Biopsy puncher, Miltex, Plainsboro, New Jersey) for the hydraulic pressure. The upper layer section and the lower layer wafer (with PDMS) were then exposed to an air plasma (1 min, 0.5 mbar, PDC-002, Harrick Plasma, Brindley, Ithaca) to allow bonding and aligned under a microscope by hand. After 80 °C for 2 h, the two bonded PDMS layers were removed from the wafer and 1.5 mm fluidic access holes were punched. To complete the device and seal the fluidic channels, 170 ± 10 µm glass coverslips were bonded to the lower side using the same air plasma and left for 30 min at 60 °C.

Operation of the microfluidic device for complete fluid exchange

Using centrifugation (900 x g, 10 min) the upper and lower layers were filled with the same solution with which the GUVs were prepared. This ensured a bubble-free environment within the channel network. Delivery of GUV suspension and solutions from a reservoir attached to the microfluidic device was achieved using a syringe pump in withdrawal mode (neMESYS, cetoni, Korbußen, Germany). After loading the device with GUVs (5-10 µl/min, 15-30 min), the valves were closed (3 bar from a custom pressure controller) for at least 1 h prior to imaging to prevent fluidic shear and allow the GUVs to reach equilibrium. With the valve still closed, the GUV suspension in the reservoir was exchanged for the desired external vesicle solution and sucked into the device (20 µl/min, 5 min). The flow rate was subsequently reduced to 2 µl/min and the valves

were opened for 2 s. After the exchange, the valves were closed once more to allow the GUVs to reach equilibrium and imaging was performed after at least 1 h.

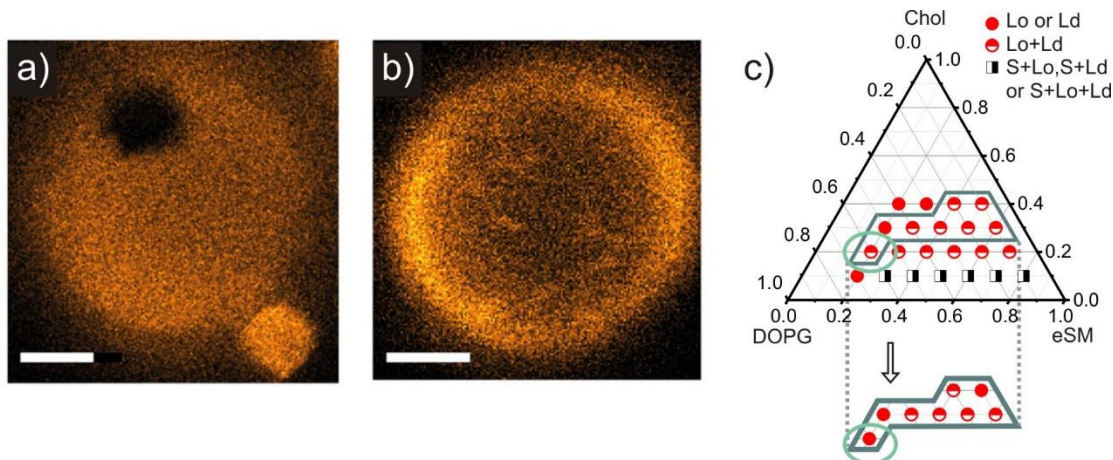**Phase-separated to homogenous membrane via complete external solution exchange**

Figure S1. Confocal images of a single GUV (DOPG/eSM/Chol 60/20/20) captured within a microfluidic device. (a) Image of the vesicle with symmetric salt/salt (in/out) showing Lo/Ld phase coexistence. (b) Image of the vesicle after a full exchange of the external solution to salt/sucrose (in/out) when the vesicle exhibited a single-liquid state. Scale bars: 2 μm. (c) Phase diagram (as in Fig. 1C in the main text) for symmetric salt/salt conditions; the lower polygonal section is obtained for asymmetric salt/sucrose (in/out) conditions after twentyfold dilution with sucrose solution. The composition of the vesicle shown in (a, b) is encircled.

References of Supplementary Information

1. Dimova, R., S. Aranda, N. Bezlyepkina, V. Nikolov, K. A. Riske, and R. Lipowsky. 2006. A practical guide to giant vesicles. Probing the membrane nanoregime via optical microscopy. J. Phys.: Condens. Matter 18:S1151-S1176.
2. Robinson, T., P. Kuhn, K. Eyer, and P. S. Dittrich. 2013. Microfluidic trapping of giant unilamellar vesicles to study transport through a membrane pore. Biomicrofluidics 7.